Observational Study

Medicine®

OPEN

Retrospective analysis of the utility of multiparametric MRI for differentiating between benign and malignant breast lesions in women in China

Wei Xiong Fan, BS[a,*], Xiao Feng Chen, MS[a], Feng Yan Cheng, MS[a], Ya Bao Cheng, BS[a], Tai Xu, BS[b], Wen Biao Zhu, MS[c], Xiao Lei Zhu, MD[d], Gui Jin Li, BS[d], Shuai Li, MD[d]

Abstract

We explored the utility of time-resolved angiography with interleaved stochastic trajectories dynamic contrast-enhanced magnetic resonance imaging (TWIST DCE-MRI), readout segmentation of long variable echo-trains diffusion-weighted magnetic resonance imaging- diffusion-weighted magnetic resonance imaging (RESOLVE-DWI), and echo-planar imaging- diffusion-weighted magnetic resonance imaging (EPI-DWI) for distinguishing between malignant and benign breast lesions.

This retrospective analysis included female patients with breast lesions seen at a single center in China between January 2016 and April 2016. Patients were allocated to a benign or malignant group based on pathologic diagnosis. All patients received routine MRI, RESOLVE-DWI, EPI-DWI, and TWIST DCE-T1WI. Variables measured included quantitative parameters (K^{trans}, K_{ep}, and V_e), semiquantitative parameters (rate of contrast enhancement for contrast agent inflow [W-in], rate of contrast decay for contrast agent outflow [W-out], and time-to-peak enhancement after contrast agent injection [TTP]) and apparent diffusion coefficient (ADC) values for RESOLVE-DWI (ADCr) and EPI-DWI (ADCe). Receiver-operating characteristic (ROC) curve analysis was used to evaluate the diagnostic utility of each parameter for differentiating malignant from benign breast lesions.

A total of 87 patients were included (benign, n = 20; malignant, n = 67). Compared with the benign group, the malignant group had significantly higher K^{trans}, K_{ep} and W-in and significantly lower W-out, TTP, ADCe, and ADCr (all $P < .05$); V_e was not significantly different between groups. RESOLVE-DWI was superior to conventional EPI-DWI at illustrating lesion boundary and morphology, while ADCr was significantly lower than ADCe in all patients. K_{ep}, W-out, ADCr, and ADCe showed the highest diagnostic efficiency (based on AUC value) for differentiating between benign and malignant lesions. Combining 3 parameters (K_{ep}, W-out, and ADCr) had a higher diagnostic efficiency (AUC, 0.965) than any individual parameter and distinguished between benign and malignant lesions with high sensitivity (91.0%), specificity (95.0%), and accuracy (91.9%).

An index combining K_{ep}, W-out, and ADCr could potentially be used for the differential diagnosis of breast lesions.

Abbreviations: ADC = apparent diffusion coefficient, ADCe = apparent diffusion coefficient for EPI-DWI (echo-planar imaging-diffusion-weighted magnetic resonance imaging) sequence, ADCr = apparent diffusion coefficient for RESOLVE-DWI (readout segmentation of long variable echo-trains diffusion-weighted magnetic resonance imaging) sequence, AUC = area under the receiver operating characteristic curve, DCE-MRI = dynamic contrast-enhanced magnetic resonance imaging, DWI = diffusion-weighted magnetic resonance imaging, EPI = echo-planar imaging, FOV = field of view, K_{ep} = transport rate describing the return of the contrast agent from the extravascular–extracellular space to the blood plasma, K^{trans} = rate of contrast agent transport from the blood plasma to the extravascular–extracellular space, MR = magnetic resonance, MRI = magnetic resonance imaging, RESOLVE-DWI = readout segmentation of long variable echo-trains diffusion-weighted magnetic resonance imaging, ROC = receiver operating characteristic, ROI = region of interest, SD = standard deviation, T2WI = T2-weighted imaging, TE = echo time, TI = inversion time, TR = repetition time, TTP = time-to-peak enhancement after contrast agent injection, TWIST = time-resolved angiography with interleaved stochastic trajectories, V_e = fractional volume of the extravascular–extracellular space in the tissue, W-in = rate of contrast enhancement for contrast agent inflow, W-out = rate of contrast decay for contrast agent outflow.

Keywords: breast lesion, diagnostic efficacy, DWI, multiparameter, quantitative dynamic enhancement

Editor: Michael Albert Thomas.

The authors have no conflicts of interest to disclose.

[a] Department of Magnetic Resonance, [b] Department of Breast Surgery, [c] Department of Pathology, Meizhou People's Hospital, Guangdong Province, [d] Siemens Healthcare NEA DI MR Application, Guangzhou, China.

[*] Correspondence: Wei Xiong Fan, Department of Magnetic Resonance, Meizhou People's Hospital, Guangdong Province 514031, China (e-mail: mrifwx@163.com).

Medicine (2018) 97:4(e9666)

Received: 10 August 2017 / Received in final form: 28 December 2017 / Accepted: 29 December 2017

http://dx.doi.org/10.1097/MD.0000000000009666

1. Introduction

Worldwide, breast cancer is the most commonly diagnosed cancer in women, and this disease accounts for 23% of all cancer cases and 14% of cancer-related deaths.[1] There was on average a 4.6% annual increase in the incidence of breast cancer in the urban Chinese population between 1982 and 2001, with a mortality rate of 8–10/100,000/year, ranking breast cancer as one of the leading causes of cancer-related deaths in women in China.[2–5] Early detection, diagnosis, and treatment are key factors for improving the prognosis of patients with breast cancer and reducing mortality rates. Patients with suspected breast cancer are examined by mammography, sonography, and magnetic resonance imaging (MRI). However, the sensitivity of mammography and sonography for invasive tumors is lower than that of magnetic resonance imaging (MRI) (mammography: 83.7%; sonography: 89.1%; and MRI: 94.6%).[6] Among the MRI modalities available, diffusion weighted MRI (DWI) and dynamic contrast-enhanced (DCE)-MRI play important roles in the diagnosis, differential diagnosis, and therapeutic evaluation of breast cancer.[7–10]

DWI is a noninvasive technique that generates tissue contrast based on differences in the diffusion of water molecules during a magnetic resonance (MR) pulse sequence. The diffusion parameters can be influenced by several intratissue properties such as fluid viscosity, intracellular-to-extracellular membrane flow, and structural properties. The diffusion rate is quantified using the apparent diffusion coefficient (ADC). Echo-planar imaging (EPI) during DWI enables faster image acquisition (40–100 ms per image). However, DWI imaging is subject to several limitations including low spatial resolution and low signal-to-noise ratio (partly due to the fast image acquisition techniques) as well as magnetic susceptibility artifacts, chemical shift artifacts, and motion artifacts.[11] Thus, the development and improvement of DWI has been an active area of research. One novel MRI technique is readout segmentation of long variable echo-trains DWI (RESOLVE-DWI), which is based on segment sampling of the EPI sequence in the readout direction.[12–14] Advantages of RESOLVE-DWI include shorter sampling time and echo time (TE) and a reduction in magnetic susceptibility artifacts, motion-induced artifacts, and blurring due to T2 decay; these advantages improve image quality and signal-to-noise ratio.[12–14]

DCE-MRI assesses perfusion and oxygenation within tumor tissue. This technique involves the intravenous injection of low-molecular weight, paramagnetic contrast agents, and the subsequent acquisition of images every few seconds for 1 to 3 minutes. Several studies have combined DWI and DCE-MRI for better assessment of breast tumors.[15–17] The semiquantitative analysis performed in DCE-MRI involves the measurement of contrast parameters from the dynamic time-signal intensity curve. However, this method cannot accurately reflect variation in the concentration of a contrast agent within a lesion. Quantitative DCE-MRI has an advantage over semiquantitative DCE-MRI in that it obtains quantitative hemodynamic parameters by dynamically monitoring the in vivo pharmacokinetics of the contrast agent through measurements of several parameters, including K^{trans} (the rate of contrast agent transport from the blood plasma to the extravascular–extracellular space), K_{ep} (the transport rate describing the return of the contrast agent from the extravascular–extracellular space to the blood plasma) and V_e (the fractional volume of the extravascular–extracellular space in the tissue). However, an important limitation of quantitative DCE-MRI is its low temporal resolution. This has been partly addressed by newer DCE-MRI techniques such as time-resolved angiography with interleaved stochastic trajectories (TWIST),[18] which increases the scanning speed by filling the *k*-space with a spiral orbit. The parameters obtained using TWIST are thought to accurately reflect blood flow and vascular permeability in the body. TWIST DCE-MRI sequences have also been shown to improve both the signal-to-noise ratio and fat-suppression, improving overall image quality by more clearly delineating lesion edges and better displaying the characteristics of internal structures.[15,19–23]

Only a small number of clinical investigations have described the use of TWIST DCE-MRI and RESOLVE-DWI in the imaging of breast diseases. Furthermore, very few studies have examined whether the combined use of TWIST DCE-MRI and RESOLVE-DWI could improve the differential diagnosis of benign and malignant breast lesions. Therefore, the present study was carried out to determine whether TWIST DCE-MRI and RESOLVE-DWI could potentially be used in the clinical setting to identify breast cancer lesions and distinguish between benign and malignant breast lesions.

2. Methods

2.1. Patients

This was a retrospective diagnostic study of patients (all females) presenting with breast lesions identified by clinical palpation, ultrasonography, or mammography. Data collection and MR scanning were performed in the People's Hospital, Meizhou, Guangdong Province, China between January 2016 and April 2016. All patients provided informed written consent before examination. The study was approved by the ethics committee of our hospital. Due to the retrospective nature of the study, consent for inclusion in the analysis was not deemed to be required.

The inclusion criteria were: biopsy, surgery, radiotherapy, chemotherapy, hormone therapy, or targeted therapy had not been undertaken before the imaging investigations were carried out; the images obtained by MR scanning contained no obvious motion artifacts and enhanced MRI yielded in-focus images; and the diagnosis was confirmed by pathologic examination of a surgically obtained specimen within 5 days of MR scanning. The exclusion criteria were: the patient had received surgical or medical treatment before the imaging examination; the patient was pregnant or in lactation; or severe heart, liver or kidney disease, immune diseases, or any other internal or surgical disease.

2.2. Instruments and methods

Imaging was carried out using a 3.0T MR scanner (Magnetom Skyra, Siemens, Germany) with dedicated, 16-channel, bilateral breast phased array coils. The patients were scanned in the prone position with the breasts unsupported. The scanned region included the bilateral breast tissue, bilateral axillae, and aorta.

The scanning parameters used for T2-weighted imaging (T2WI) were: repetition time (TR), 3570 ms; TE, 74 ms; inversion time (TI), 230 ms; slice thickness, 4.0 mm; spacing between slices, 0.4 mm; field of view (FOV), 341 × 341 mm; acquisition matrix, 314 × 448. The parameters for EPI-DWI were: TR, 4200 ms; TE, 62 ms; *b*-value, 0, 50, or 800 s/mm^2; FOV, 149 × 340 mm; acquisition matrix, 86 × 220; slice thickness, 4.0 mm; spacing between slices, 0.8 mm. The parameters for RESOLVE-DWI were: TR, 4800 ms; TE, 562 ms; *b*-value, 0 or 800 s/mm^2; FOV,

170 × 340 mm; acquisition matrix, 96 × 192; slice thickness, 4.0 mm; spacing between slices, 0.8 mm. The parameters for T1WI were: TR, 5.5 ms; TE, 2.5 ms; FOV, 341 × 341 mm; acquisition matrix, 426 × 448; slice thickness, 1.5 mm; spacing between slices, 0.3 mm. The parameters for T1 DCE-MRI sequences were: TR, 6.4 ms; TE, 3.3 ms; FOV, 288 × 384 mm; acquisition matrix, 288 × 384; slice thickness, 2.0 mm; spacing between slices, 0.4 mm. TWIST technology was used for dynamic enhanced scanning; the MR contrast agent (Gd-DTPA, 0.2 mmol/kg body weight) was injected at a rate of 3.0 mL/s, and an additional 20 mL of saline was then injected at the same rate. Scanning was nonintermittent with a total of 34 scan phases. The scanning time was 17.7 s for the first phase and 8.7 s for all subsequent phases; the total scan time was 5 minutes and 5 seconds (304.8 seconds).

2.3. MRI data processing and collection

All images were analyzed and processed independently by 2 attending radiologists who had more than 5 years of work experience. Differences of opinion were resolved by discussion. The image was transmitted to a Syngo Via workstation (Siemens) and postprocessing was carried out using Tissue 4D software (Siemens). The lesion location was confirmed using a combination of T2WI, DWI, and enhanced imaging. The most clearly enhanced region in the lesion was selected as the region of interest (ROI). The Tofts model was used to measure and calculate the following quantitative parameters for each lesion: the volume transfer constant, K^{trans} (min^{-1}), which is the rate constant for the diffusion of the contrast agent from the intravascular to the extravascular space; the extravascular–extracellular space volume ratio, V_e, which is the extravascular–extracellular space volume for the entire voxel ratio; and K_{ep} (min^{-1}), which is the rate constant for the diffusion of the contrast agent from the extravascular to the intravascular space. The relationship between the 3 parameters was: $V_e = K^{trans}/K_{ep}$. Pseudocolor images of the quantitative parameters and the time-concentration curve were obtained. The following semiquantitative parameters for each lesion were derived using a qualitative model: the rate of contrast enhancement for contrast agent inflow (W-in) (min^{-1}); the rate of contrast decay for contrast agent outflow (W-out) (min^{-1}); and the time-to-peak enhancement after contrast agent injection (TTP) (minutes). Pseudocolor images and the time-concentration curve were obtained for each semiquantitative parameter. The RESOLVE-DWI sequence ($b = 800$), EPI-DWI sequence ($b = 800$) and their respective ADC images were opened as read-only files, and the ADC values for the RESOLVE-DWI sequence (ADCr) and EPI-DWI sequence (ADCe) were measured in the same region of the lesion. To avoid measurement error, the ROI was selected so as to avoid blood vessels, regions of calcification, fatty tissue, cavities and necrotic tissue. Each lesion parameter was measured 3 times with the region in which the measurement was made kept as consistent as possible, and the averaged value was taken as the final measurement.

2.4. Gold standard

The cases were divided into 2 groups (benign group or malignant group) based on the pathologic results, which were considered as the gold standard.

2.5. Statistical analysis

SPSS 17.0 software (IBM, Armonk, NY) was used for data analysis. The data for each parameter were subjected to tests of normality and homogeneity of variance. Quantitative data are presented as means ± standard deviations (SDs) and categorical data are presented as frequencies and percentages. For parameters that were normally distributed and had homogeneity of variance, the independent-samples *t*-test was used for comparisons between groups. For parameters that were non-normally distributed or showed heterogeneity of variance, a nonparametric test for 2 independent samples (rank sum test) was applied. The difference between ADCr and ADCe was normally distributed, so a paired-sample *t*-test was used for comparisons between the 2 groups. Receiver operating characteristic (ROC) curve analysis was used to evaluate the diagnostic utility of each parameter for the detection of malignant breast lesions. The area under the curve (AUC), diagnostic threshold, sensitivity, specificity, and diagnostic accuracy of each parameter were calculated according to the maximum Youden index (Youden index = sensitivity + specificity − 1). The diagnostic efficiency of combining quantitative DCE-MRI parameters with the ADC value was also investigated. A P-value $< .05$ was considered to indicate statistical significance.

3. Results

3.1. Baseline clinical characteristics of the study participants

A total of 89 lesions (2 cases with double lesions) from 87 patients (all females) satisfied the inclusion and exclusion criteria. The benign group (age range, 36–69 years; median age, 46 years) consisted of 20 patients with 21 lesions, including fibroadenoma (n = 7), intraductal papilloma (n = 5), mammary dysplasia (n = 3), adenosis of the breast (n = 2), benign phyllodes tumor (n = 2), sclerosing adenosis (n = 1), and chronic nonspecific mastitis (n = 1). The malignant group (age range, 25–79 years; median age, 48 years) comprised 67 patients with 68 lesions, including invasive ductal carcinoma (n = 55), preinvasive carcinoma (n = 5), intraductal carcinoma accompanied by microinvasion (n = 4), medullary carcinoma (n = 2), malignant grade II phyllodes tumor (n = 1), and mucinous carcinoma (n = 1). One lesion from each of the benign and malignant groups was excluded from further analysis due to parameter deviation; therefore, a total of 87 cases with 87 lesions (20 in the benign group, 67 in the malignant group) were included in the final analysis. There were no significant differences between the malignant and benign groups in patient age, weight, or family history of breast cancer (Table 1).

3.2. Image quality assessment

No obvious motion artifacts were observed in any of the images from the 87 patients. The lesions could be clearly observed in

Table 1

Comparison of baseline clinical data between the benign and malignant groups.

	Malignant group	Benign group	*T* or χ^2 value	*P* value
N	67	20		
Age (years), mean ± SD	49.53 ± 1.36	47.29 ± 2.28	0.713*	.478
Weight (kg), mean ± SD	59.70 ± 0.79	62.21 ± 1.69	−1.341*	.184
Family history of breast cancer, n (%)	21 (31.3%)	2 (10.0%)	1.995†	.136

SD = standard deviation.
* *T* value (independent-samples t-test).
† χ^2 value (chi-squared test).

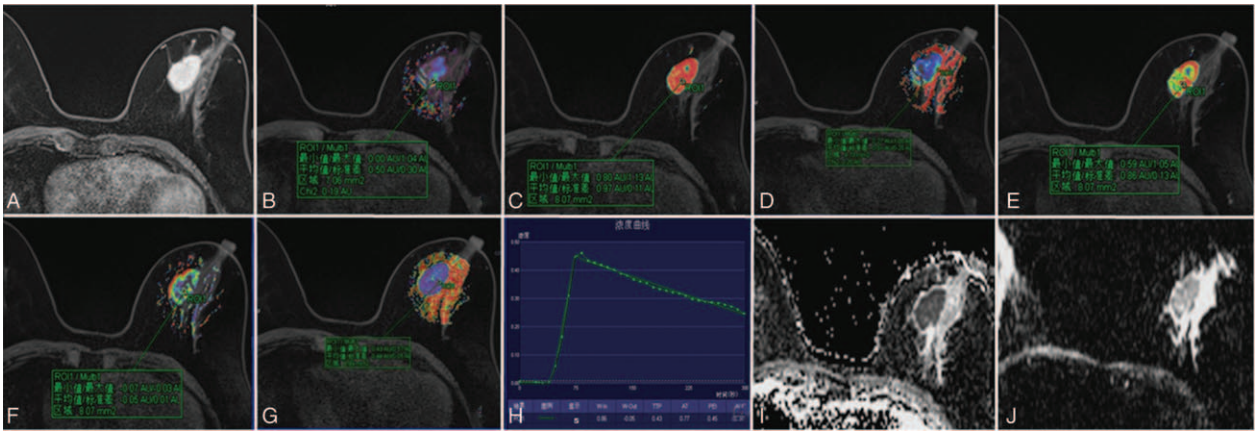

Figure 1. Representative MR images from a patient with infiltrating ductal carcinoma (grade III). (A) TWIST-DCE image. (B–G) pseudocolor images for K^{trans} (B), K_{ep} (C), V_e (D), W-in (E), W-out (F), and TTP (G). Red represents high values, yellow intermediate values, and blue low values. The values for K^{trans}, K_{ep}, V_e, W-in, W-out, and TTP were 0.50 min^{-1}, 0.99 min^{-1}, 0.45, 0.86 min^{-1}, −0.05 min^{-1}, and 0.43 minutes, respectively. (H) Concentration–time curve for the ROI. (I) ADC image for RESOLVE-DWI. (J) ADC image for conventional EPI-DWI. ADC= apparent diffusion coefficient, DCE=dynamic contrast-enhanced, EPI=echo-planar imaging, K_{ep}=transport rate describing the return of the contrast agent from the extravascular–extracellular space to the blood plasma, K^{trans}=rate of contrast agent transport from the blood plasma to the extravascular–extracellular space, MR=magnetic resonance, RESOLVE-DWI=readout segmentation of long variable echo-trains diffusion-weighted magnetic resonance imaging, ROI=region of interest, TTP=time-to-peak enhancement after contrast agent injection, TWIST=time-resolved angiography with interleaved stochastic trajectories, V_e= fractional volume of the extravascular–extracellular space in the tissue, W-in=rate of contrast enhancement for contrast agent inflow, W-out=rate of contrast decay for contrast agent outflow.

DCE-MRI or DWI sequences. TWIST DCE-MRI yielded images with a higher signal-to-noise ratio that clearly delineated the lesion margins and revealed the characteristics of the lesion's internal structure. The RESOLVE-DWI sequence and its ADC image were superior to the EPI-DWI sequence and its ADC image at showing the morphology of the lesion and its boundary (Fig. 1).

3.3. Analysis of quantitative and semiquantitative parameters

The mean values of the quantitative parameters K^{trans} and K_{ep} were significantly higher in the malignant group than in the benign group (K^{trans}: 0.154 ± 0.015 vs $0.091 \pm 0.014\,min^{-1}$, $P=.036$; K_{ep}: 0.947 ± 0.089 vs $0.441 \pm 0.065\,min^{-1}$, $P=.001$), whereas V_e was not significantly different between groups (Table 2). With regard to the semiquantitative parameters, the mean value of W-in was significantly higher in the malignant group than in the benign group (0.638 ± 0.0364 vs 0.379 ± 0.074 min^{-1}, $P=.002$) while the mean values of W-out (-0.023 ± 0.012 vs $0.022 \pm 0.006\,min^{-1}$, $P<.001$) and TTP (0.639 ± 0.034 vs 1.276 ± 0.165 minutes, $P<.001$) were significantly lower in the malignant group than in the benign group (Table 2).

Both the RESOLVE-DWI ($b=800$) and EPI-DWI ($b=800$) sequences exhibited a higher or slightly higher signal in the

Table 2

Comparison of parameters and apparent diffusion coefficient values between the malignant and benign groups.

Parameter	Malignant group (n=67)	Benign group (n=20)	*P* value
K^{trans} (min^{-1}), mean±SD	0.154±0.015	0.091±0.014	.036
95% confidence interval	0.124–0.184	0.062–0.121	
K_{ep} (min^{-1}), mean±SD	0.947±0.089	0.441±0.065	.001
95% confidence interval	0.770–1.124	0.300–0.581	
V_e, mean±SD	0.187±0.016	0.246±0.052	.183
95% confidence interval	0.155–0.219	0.134–0357	
W-in (min^{-1}), mean±SD	0.638±0.0364	0.379±0.074	.002
95% confidence interval	0.560–0.707	0.218–0.540	
W-out (min^{-1}), mean±SD	−0.023±0.012	0.022±0.006	<.001
95% confidence interval	−0.048–0.001	0.009–0.035	
TTP minutes, mean±SD	0.639±0.034	1.276±0.165	
95% confidence interval	0.572–0.706	0.921–1.632	<.001
ADCr ($\times 10^{-3}$ mm^2/s), mean±SD	0.776±0.016	1.226±0.075	
95% confidence interval	0.743–0.809	1.063–1.390	<.001
ADCe ($\times 10^{-3}$ mm^2/s), mean±SD	0.838±0.019	1.375±0.110	
95% confidence interval	0.800–0.876	1.137–1.613	<.001

ADCe=apparent diffusion coefficient for EPI-DWI (echo-planar imaging- diffusion-weighted magnetic resonance imaging) sequence, ADCr=apparent diffusion coefficient for RESOLVE-DWI (readout segmentation of long variable echo-trains diffusion-weighted magnetic resonance imaging) sequence, K_{ep}=transport rate describing the return of the contrast agent from the extravascular–extracellular space to the blood plasma, K^{trans}=rate of contrast agent transport from the blood plasma to the extravascular–extracellular space, SD=standard deviation, TTP=time to peak enhancement after contrast agent injection, V_e=fractional volume of the extravascular–extracellular space in the tissue, W-in=rate of contrast enhancement for contrast agent inflow, W-out=rate of contrast decay for contrast agent outflow.

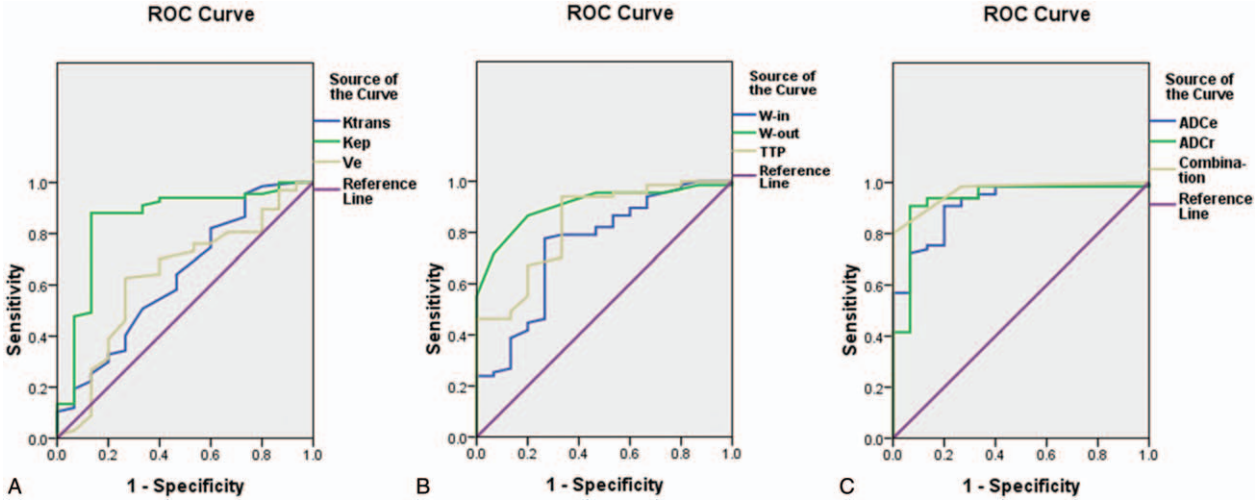

Figure 2. ROC curves for each parameter. (A) ROC curves for the quantitative parameters K^{trans}, K_{ep}, and V_e. (B) ROC curves for the semiquantitative parameters W-in, W-out, and TTP. (C) ROC curves for ADCr and ADCe. ADCe = apparent diffusion coefficient for EPI-DWI (echo-planar imaging-diffusion-weighted magnetic resonance imaging) sequence, ADCr = apparent diffusion coefficient for RESOLVE-DWI (readout segmentation of long variable echo-trains diffusion-weighted magnetic resonance imaging) sequence, K_{ep} = transport rate describing the return of the contrast agent from the extravascular–extracellular space to the blood plasma, K^{trans} = rate of contrast agent transport from the blood plasma to the extravascular–extracellular space, ROC = receiver operating characteristic, TTP = time-to-peak enhancement after contrast agent injection, V_e = fractional volume of the extravascular–extracellular space in the tissue, W-in = rate of contrast enhancement for contrast agent inflow, W-out = rate of contrast decay for contrast agent outflow.

malignant group than in the benign group. The mean values of ADCr and ADCe were significantly lower in the malignant group than in the benign group (ADCr: 0.776 ± 0.016 vs $1.226 \pm 0.075 \times 10^{-3}\,mm^2/s$, $P < .001$; ADCe: 0.838 ± 0.019 vs $1.375 \pm 0.110 \times 10^{-3}\,mm^2/s$, $P < .001$; Table 2). In addition, the mean value of ADCr in all patients ($0.883 \pm 0.033 \times 10^{-3}\,mm^2/s$) was significantly lower than that of ADCe ($0.957 \pm 0.038 \times 10^{-3}\,mm^2/s$; $P < .001$).

3.4. Diagnostic utility of each parameter for distinguishing malignant from benign breast lesions

The ROC curves for each parameter are shown in Figure 2. The optimal critical threshold and the corresponding sensitivity and specificity values for each parameter were obtained through determination of the maximum Youden index (Fig. 2, Table 3). The AUC was higher for K_{ep} (0.890) than for K^{trans} (0.679) or V_e (0.613), suggesting that K_{ep} had the highest diagnostic efficiency among the quantitative parameters (Table 3). The optimal threshold value for K_{ep} was 0.580 min^{-1}, and this resulted in sensitivity, specificity and accuracy values of 89.6%, 90.0% and 89.6%, respectively. The AUC of W-out (0.922) was higher than that of W-in (0.751) or TTP (0.855), indicating that W-out had the highest diagnostic efficiency among the semiquantitative parameters (Table 3). With 0.005 as the optimal threshold value, the sensitivity, specificity, and accuracy of W-out were 89.6%, 85.0%, and 88.5%, respectively. The AUCs of ADCr (0.943) and ADCe (0.924) were both high, suggesting high diagnostic efficiency (Table 3). Using $0.929 \times 10^{-3}\,mm^2/s$ as the optimal threshold, the sensitivity, specificity, and accuracy of ADCr were 92.5%, 90.0%, and 91.9%, respectively.

Table 3

Diagnostic efficiency, sensitivity, specificity and accuracy of the various parameters for distinguishing malignant from benign breast lesions.

Parameter	AUC	Maximum Youden index	Optimal threshold	Sensitivity (%)	Specificity (%)	Accuracy (%)
K^{trans}	0.679	0.286	0.075	83.6	45.0	74.7
K_{ep}	0.890	0.796	0.580	89.6	90.0	89.6
V_e	0.613	0.327	0.175	62.7	70.0	64.4
W-in	0.751	0.491	0.445	79.1	70.0	77.0
W-out	0.922	0.746	0.005	89.6	85.0	88.5
TTP	0.855	0.655	1.045	95.5	70.0	89.6
ADCr	0.943	0.825	0.929	92.5	90.0	91.9
ADCe	0.924	0.725	0.994	92.5	80.0	89.7
Combined index	0.965	0.860	2	91.0	95.0	91.9

Note: K_{ep}, W-out, and ADCr were used for the combined diagnostic index. ADCe = apparent diffusion coefficient for EPI-DWI (echo-planar imaging- diffusion-weighted magnetic resonance imaging) sequence, ADCr = apparent diffusion coefficient for RESOLVE-DWI (readout segmentation of long variable echo-trains diffusion-weighted magnetic resonance imaging) sequence, K_{ep} = transport rate describing the return of the contrast agent from the extravascular–extracellular space to the blood plasma, K^{trans} = rate of contrast agent transport from the blood plasma to the extravascular–extracellular space, SD = standard deviation, TTP = time-to-peak enhancement after contrast agent injection, V_e = fractional volume of the extravascular–extracellular space in the tissue, W-in = rate of contrast enhancement for contrast agent inflow, W-out = rate of contrast decay for contrast agent outflow.

3.5. Diagnostic utility of a combined diagnostic index for distinguishing malignant from benign breast lesions

The quantitative parameter K_{ep} and the semiquantitative parameters W-out and ADCr were selected for the combined diagnostic index, since these showed the highest diagnostic efficiency among their respective parameter groups. The combined index was calculated as follows: 1 point was assigned for each of $K_{ep} \geq 0.580\ min^{-1}$, W-out ≤ 0.005, and ADCr $\leq 0.929 \times 10^{-3}\ mm^2/s$; a score of ≥ 2 points (i.e., at least 2 of these criteria were met) was taken to indicate a malignant lesion. The sensitivity, specificity, and accuracy of this combined index were 91.0%, 95.0%, and 91.9%, respectively (Fig. 2, Table 3). Furthermore, the AUC of the combined index was 0.965, higher than that of any individual parameter.

4. Discussion

In this retrospective study, we have compared the utilities of several quantitative (K^{trans}, K_{ep}, V_e) and semiquantitative (W-in, W-out, TTP, ADCr, and ADCe) parameters for distinguishing between benign and malignant breast lesions. We found that K_{ep}, W-out, ADCr, and ADCe showed the highest diagnostic efficiency (based on AUC value) for differentiating between benign and malignant breast lesions. Furthermore, the combination of 3 diagnostic parameters (K_{ep}, W-out, and ADCr) had a diagnostic efficiency (AUC value of 0.965) greater than that of any individual parameter and could distinguish between benign and malignant breast lesions with high sensitivity, specificity, and accuracy (91.0%, 95.0%, and 91.9%, respectively). This combined index could potentially be used in the clinic for the differential diagnosis of breast lesions.

The occurrence, development, and outcome of tumors is closely related to angiogenesis.[12] During the development of breast cancer, the secretion of a variety of vasoactive substances leads to increases in tumor microvessel density and alterations in the volume and flow of blood in the tumor microcirculation. Structural disorders in the newly formed blood vessels, immaturity of the vascular endothelial cells, and basement membrane and increased vascular permeability all contribute to an imbalance in the microcirculation of a breast cancer lesion.[24,25] DCE-MRI measures the characteristics of the microvascular perfusion of a lesion, and thus can potentially distinguish between benign and malignant tissues. We found that the DCE-MRI quantitative parameters, K^{trans} and K_{ep}, were significantly increased in malignant breast lesions, consistent with numerous previous studies.[19,26–29] We speculate that the enhancement of malignant tumors with contrast agent is increased (relative to that of benign tumors) due to the presence of a high density of new vessels with structural disorders that have an elevated permeability. In our study, the diagnostic efficacy of K_{ep} was higher than that of K^{trans}, with the former having a high sensitivity and specificity and the latter a high sensitivity but low specificity. The lower specificity for K^{trans} could arise due to the fact that this parameter is influenced by changes in the blood flow of the supplying blood vessel, the transmembrane velocity of the contrast agent and the diffusion rate in the intercellular space. Thus, K_{ep} may be a more stable parameter than K^{trans}, as shown in a previous study.[30] However, the range of K^{trans} and K_{ep} values obtained for benign and malignant lesions in our study was different from values reported previously.[19,26–29,31] One possible reason for this apparent discrepancy is that the various studies used different mathematical models, which would have resulted in different values for the hemodynamic parameters.[32] In addition, the scanning sequences and doses of contrast agent used during scanning also differed between studies and thus may have contributed to variations in the calculated values of the parameters. Despite differences in the absolute values of the parameters, a consistent finding in our study and these previous investigations[19,26–29] was that the K^{trans} and K_{ep} values were significantly higher for malignant breast lesions than for benign lesions.

Although this study found that V_e was numerically lower in the malignant group than in the benign group, this difference was not significant as suggested in previous studies.[28,31] In contrast, Dou et al[28] showed that V_e was reduced successively from malignant lesions to benign lesions to normal tissue, whereas we observed that V_e was lower in the malignant group than in the benign group. Another study also observed that the V_e value was unstable,[33] and it was suggested that V_e may be affected by edema around the lesion or gradual changes in the relative proportions of extravascular volume and extracellular volume in the tissue during the development of the lesion. Variations in the results between studies may also be due to differences in the input artery;[34,35] however, the specific reasons for the apparent discrepancies between investigations require further research.

Comparisons of semiquantitative parameters (W-in, W-out, and TTP) between malignant and benign lesions revealed that malignant lesions exhibited faster inflow and outflow of contrast agent with a shorter time to achieve the peak contrast agent concentration. These differences between malignant and benign lesions may arise from increased vascular permeability and enhanced delivery/exchange of contrast agent in malignant lesions,[28] in turn due to a high density of newly formed blood vessels, disorganized vascular structure, increased vessel diameter induced by arteriovenous fistula formation, abnormal endothelial integrity, a thin vascular wall and reduced quantities of basement membrane.

DWI observes the Brownian motion of water molecules in vivo and provides information regarding the functional changes in water molecule movement in human tissues from a molecular angle. In malignant tumors, vigorous cell proliferation, a high cell density and a reduction in the extracellular space limit the activity of water molecules and decrease the ADC value. This study showed that the ADCe and ADCr values were significantly lower in malignant breast lesions than in benign lesions and that both these parameters had high diagnostic efficiency for distinguishing malignant lesions from benign lesions. RESOLVE-DWI was superior to conventional EPI-DWI at illustrating lesion morphology and identifying the boundary of the lesion, with no obvious image deformities or artifacts seen, suggesting that RESOLVE-DWI may have advantages over EPI-DWI in the differential diagnosis of breast lesions. The mean ADCr value in all patients was significantly lower than the ADCe value, in contrast to a previous study reporting that although the ADC value was numerically lower for RESOLVE-DWI than for conventional DWI, this apparent difference was not significant.[36] Further investigations with larger sample sizes are needed to resolve this apparent inconsistency between studies.

There were several limitations to this study. First, the parameters were compared only between benign and malignant lesions; measurements of the parameters in a normal control group (i.e., normal breast tissue) were not undertaken, and comparisons between different grades of malignant lesion were also not made. This limits the interpretation of the results. Second, the number of benign cases included in the analysis was

small, which may have influenced the statistical results. Third, our study did not analyze whether the ROI size had an impact on parameter measurement. Fourth, our analysis was retrospective and so may have been prone to selection bias, recall bias, and confounding. Prospective studies are needed to confirm and extend our observations.

TWIST DCE-MRI had high temporal and spatial resolution and could reflect the morphologic and hemodynamic features of breast lesions. Lesion shape and boundary were more clearly observed using RESOLVE-DWI than conventional EPI-DWI. Of the quantitative and semiquantitative parameters assessed, K_{ep}, W-out, ADCr, and ADCe showed the highest diagnostic efficiency for differentiating between benign and malignant breast lesions. Furthermore, the combination of 3 diagnostic parameters (K_{ep}, W-out, and ADCr) distinguished between benign and malignant breast lesions with high sensitivity, specificity, and accuracy.

References

[1] Jemal A, Bray F, Center MM, et al. Global cancer statistics. CA Cancer J Clin 2011;61:69–90.

[2] Wong IO, Schooling CM, Cowling BJ, et al. Breast cancer incidence and mortality in a transitioning Chinese population: current and future trends. Br J Cancer 2015;112:167–70.

[3] Li T, Mello-Thoms C, Brennan PC. Descriptive epidemiology of breast cancer in China: incidence, mortality, survival and prevalence. Breast Cancer Res Treat 2016;159:395–406.

[4] Wang QJ, Zhu WX, Xing XM. Analysis of the incidence and survival of female breast cancer in Beijing during the last 20 years. Zhonghua Zhong Liu Za Zhi 2006;28:208–10.

[5] Chen K, He M, Dong S, et al. Descriptive epidemiology of female breast cancer in Tianjin, China. Chin J Clin Oncol 2004;3:207–10.

[6] Malur S, Wurdinger S, Moritz A, et al. Comparison of written reports of mammography, sonography and magnetic resonance mammography for preoperative evaluation of breast lesions, with special emphasis on magnetic resonance mammography. Breast Cancer Res 2001;3:55–60.

[7] Petralia G, Bonello L, Priolo F, et al. Breast MR with special focus on DW-MRI and DCE-MRI. Cancer Imaging 2011;11:76–90.

[8] Thomassin-Naggara I, De Bazelaire C, Chopier J, et al. Diffusion-weighted MR imaging of the breast: advantages and pitfalls. Eur J Radiol 2013;82:435–43.

[9] Ei Khouli RH, Jacobs MA, Mezban SD, et al. Diffusion-weighted imaging improves the diagnostic accuracy of conventional 3.0-T breast MR imaging. Radiology 2010;256:64–73.

[10] Guo Y, Cai YQ, Cai ZL, et al. Differentiation of clinically benign and malignant breast lesions using diffusion-weighted imaging. J Magn Reson Imaging 2002;16:172–8.

[11] Chilla GS, Tan CH, Xu C, et al. Diffusion weighted magnetic resonance imaging and its recent trend-a survey. Quant Imaging Med Surg 2015;5:407–22.

[12] Porter DA, Heidemann RM. High resolution diffusion-weighted imaging using readout-segmented echo-planar imaging, parallel imaging and a two-dimensional navigator-based reacquisition. Magn Reson Med 2009;62:468–75.

[13] Ishida G, Oishi M, Morii K, et al. Application of brain diffusion-weighted imaging performed using readout segmentation of long variable echo trains. No Shinkei Geka 2015;43:31–40.

[14] Bogner W, Pinker-Domenig K, Bickel H, et al. Readout-segmented echo-planar imaging improves the diagnostic performance of diffusion-weighted MR breast examinations at 3.0 T. Radiology 2012;263:64–76.

[15] Rahbar H, Partridge SC, Demartini WB, et al. In vivo assessment of ductal carcinoma in situ grade: a model incorporating dynamic contrast-enhanced and diffusion-weighted breast MR imaging parameters. Radiology 2012;263:374–82.

[16] Wu LM, Hu JN, Gu HY, et al. Can diffusion-weighted MR imaging and contrast-enhanced MR imaging precisely evaluate and predict pathological response to neoadjuvant chemotherapy in patients with breast cancer? Breast Cancer Res Treat 2012;135:17–28.

[17] Fusco R, Sansone M, Filice S, et al. Integration of DCE-MRI and DW-MRI quantitative parameters for breast lesion classification. Biomed Res Int 2015;2015:237863.

[18] Song T, Laine AF, Chen Q. Optimal k-Space Sampling for Dynamic Contrast-Enhanced MRI with an Application to MR Renography. Magn Reson Med 2009;61:1242–8.

[19] Tudorica LA, Oh KY, Roy N, et al. A feasible high spatiotemporal resolution breast DCE-MRI protocol for clinical settings. Magn Reson Imaging 2012;30:1257–67.

[20] Lim RP, Shapiro M, Wang EY, et al. 3D time-resolved MR angiography (MRA) of the carotid arteries with time-resolved imaging with stochastic trajectories: comparison with 3D contrast-enhanced Bolus-Chase MRA and 3D time-of-flight MRA. AJNR Am J Neuroradiol 2008; 29:1847–54.

[21] Le Y, Kroeker R, Kipfer HD, et al. Development and evaluation of TWIST Dixon for dynamic contrast-enhanced (DCE) MRI with improved acquisition efficiency and fat suppression. J Magn Reson Imaging 2012;36:483–91.

[22] Hu YQ, Tao AI, Yan L, et-al. DCE-MRI with CAIPIRINHA-Dixon-TWIST-VIBE technique for breast lesions: quantitative analysis of pharmacokinetics parameters. J Diagnost Imaging Intervent Radiol 2016;2:98–101.

[23] Le Y, Kipfer H, Majidi S, et al. Application of time-resolved angiography with stochastic trajectories (TWIST)-Dixon in dynamic contrast-enhanced (DCE) breast MRI. J Magn Reson Imaging 2013;38:1033–42.

[24] Nagy JA, Chang SH, Dvorak AM, et al. Why are tumour blood vessels abnormal and why is it important to know? Br J Cancer 2009;100:865–9.

[25] McDonald DM, Baluk P. Imaging of angiogenesis in inflamed airways and tumors: newly formed blood vessels are not alike and may be wildly abnormal: Parker B. Francis lecture. Chest 2005;128(6 suppl):602s–8s.

[26] Li RM, Gu YJ, Mao J, et al. Study on quantitative dynamic contrast-enhanced MRI in differentiating benign and malignant breast lesions. Chinese J Radiol 2011;45:164–9.

[27] Medeiros LR, Duarte CS, Rosa DD, et al. Accuracy of magnetic resonance in suspicious breast lesions: a systematic quantitative review and meta-analysis. Breast Cancer Res Treat 2011;126:273–85.

[28] Dou RX, Yang L, Huang N. The clinical value and pathological control study of quantitative DCE-MRI in the diagnosis of benign and malignant breast lesions. Chin J Magn Reson Imaging 2015;8:592–8.

[29] Zhu RR, Ding J, Huang N. The application value of quantitative dynamic contrast-enhanced MRI in breast mass-like adenosis. J Pract Radiol 2016;2:208–11.

[30] Koo HR, Cho N, Song IC, et al. Correlation of perfusion parameters on dynamic contrast-enhanced MRI with prognostic factors and subtypes of breast cancers. J Magn Reson Imaging 2012;36:145–51.

[31] Huang W, Li X, Morris EA, et al. The magnetic resonance shutter speed discriminates vascular properties of malignant and benign breast tumors in vivo. Proc Natl Acad Sci U S A 2008;105:17943–8.

[32] Jiang Y, Lou J, Wang S, et al. Evaluation of the role of dynamic contrast-enhanced MR imaging for patients with BI-RADS 3–4 microcalcifications. PLoS One 2014;9:e99669.

[33] Tofts PS. Modeling tracer kinetics in dynamic Gd-DTPA MR imaging. J Magn Reson Imaging 1997;7:91–101.

[34] Wang Y, Huang W, Panicek DM, et al. Feasibility of using limited-population-based arterial input function for pharmacokinetic modeling of osteosarcoma dynamic contrast-enhanced MRI data. Magn Reson Med 2008;59:1183–9.

[35] Cheng HL. Investigation and optimization of parameter accuracy in dynamic contrast-enhanced MRI. J Magn Reson Imaging 2008;28: 736–43.

[36] Fu Y, Shi YF, Yan K, et al. Clinical value of real time elastography in patients with unexplained cervical lymphadenopathy: quantitative evaluation. Asian Pac J Cancer Prev 2014;15:5487–92.